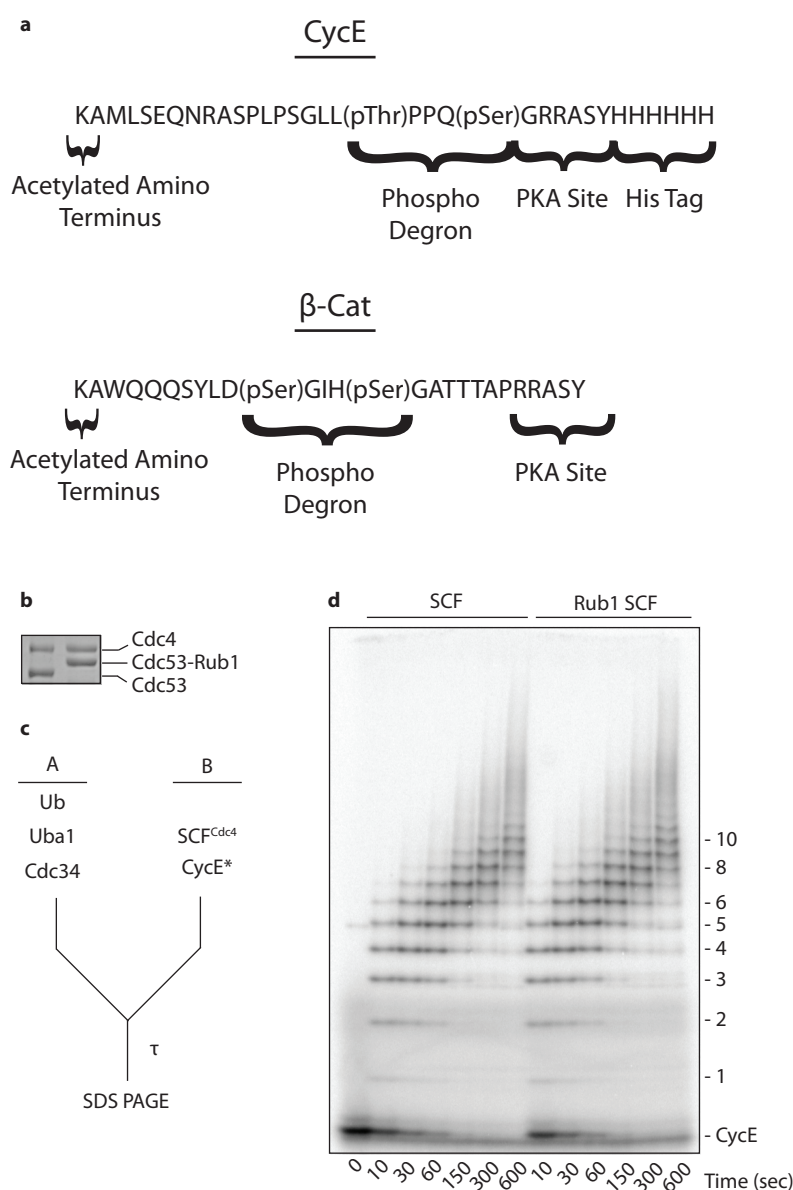
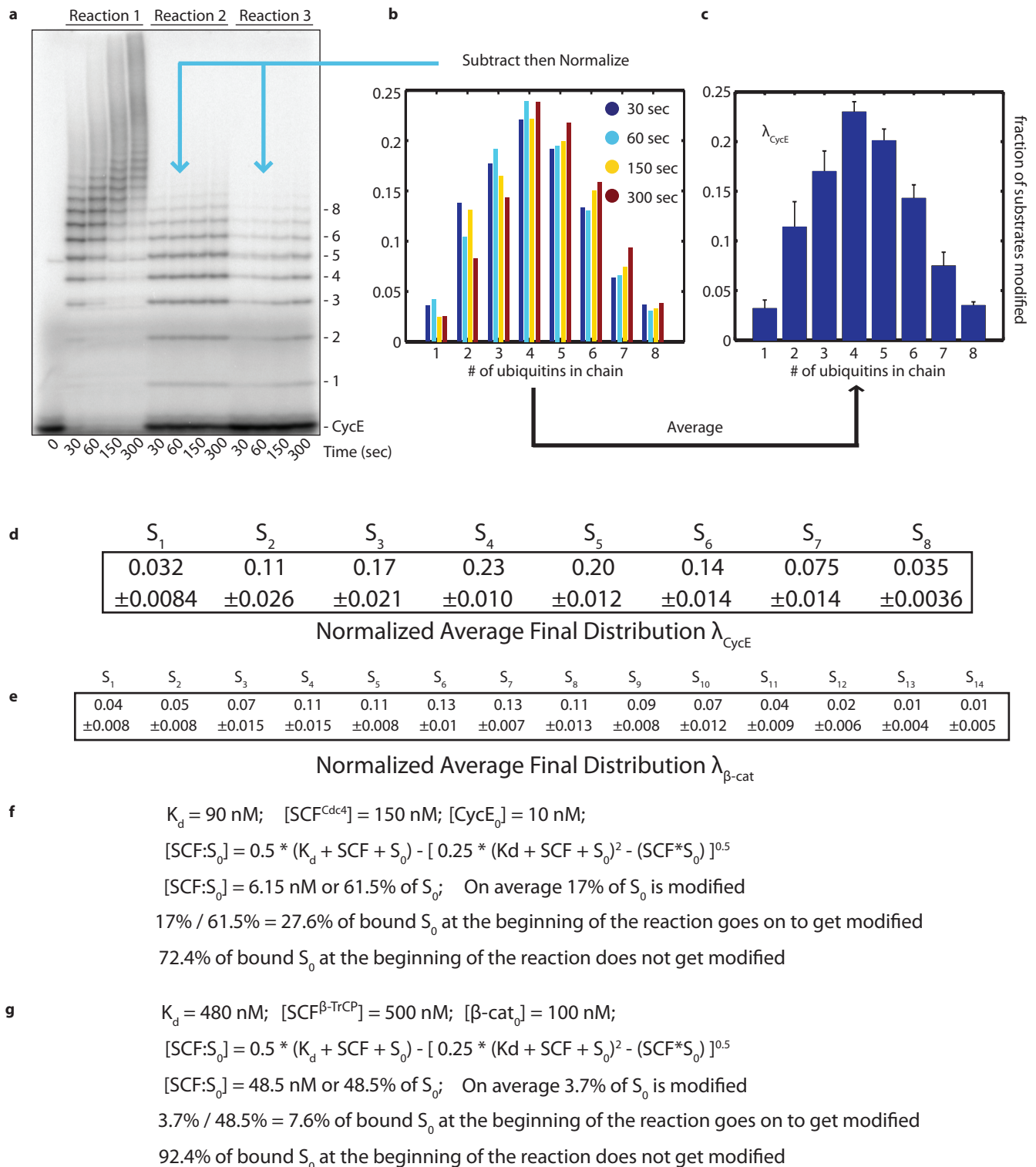


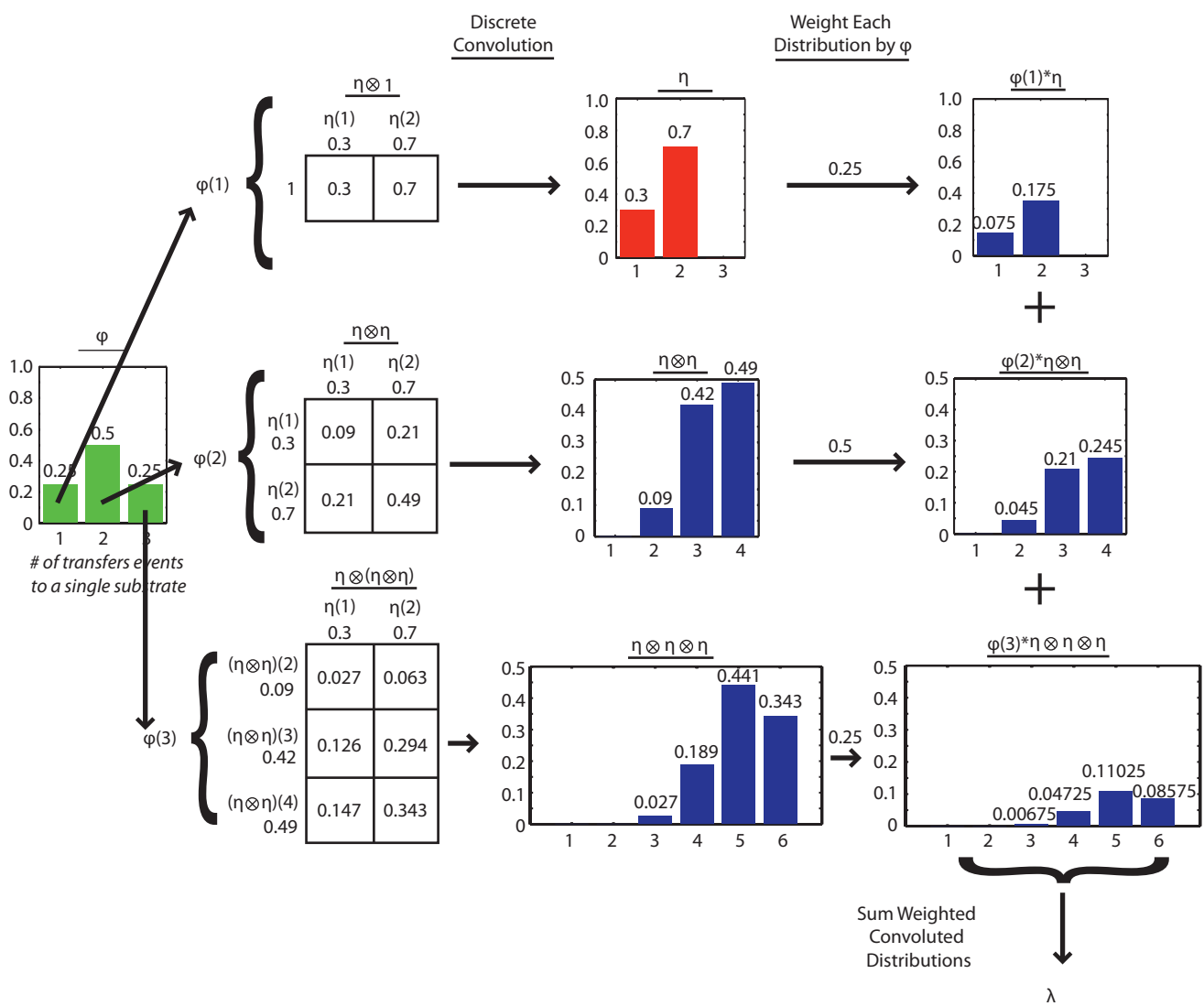
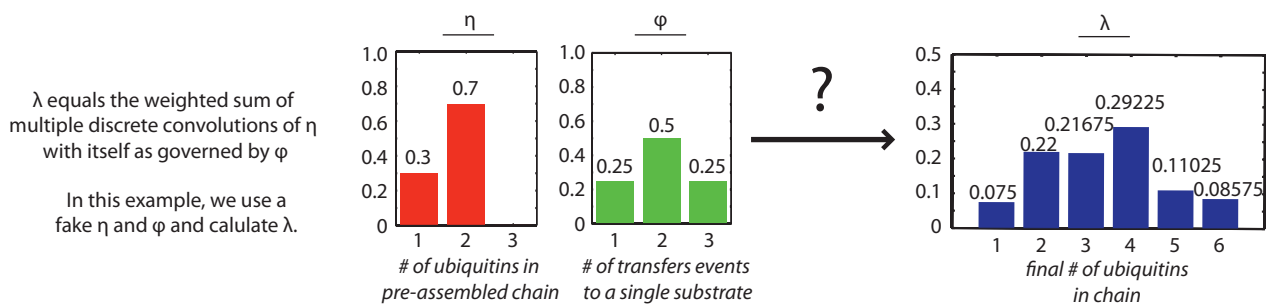
SUPPLEMENTARY INFORMATION

**Supplementary Figure 1 | Attachment of Rub1 to SCFCdc4 did not change ubiquitylation kinetics of CycE.**

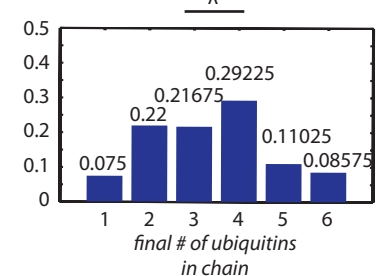
a, The design of CycE and β-Cat. The sequence from Lys1 through pSer23 is derived directly from human cyclin E1. **b**, SCFCdc4 was bound to beads coupled to the anti-Py antibody. Beads were mixed with purified Rub1, Uba1–Uba3, Ubc12, and ATP. After washing, the Rub1-conjugated SCFCdc4 was released with the Py peptide and analyzed by SDS-PAGE followed by staining with Coomassie Blue. Lane 1: unmodified SCFCdc4, lane 2: Rub1-conjugated SCFCdc4. **c**, Reaction design: SCFCdc4 or Rub1-conjugated SCFCdc4 (150 nM) was pre-mixed with 32P labeled CycE (10 nM) and combined with pre-mixed ubiquitin (60 μM), Uba1 (0.8 μM), Cdc34 (10 μM), and ATP. **d**, Reactions were evaluated by SDS-PAGE followed by phosphor-imaging.

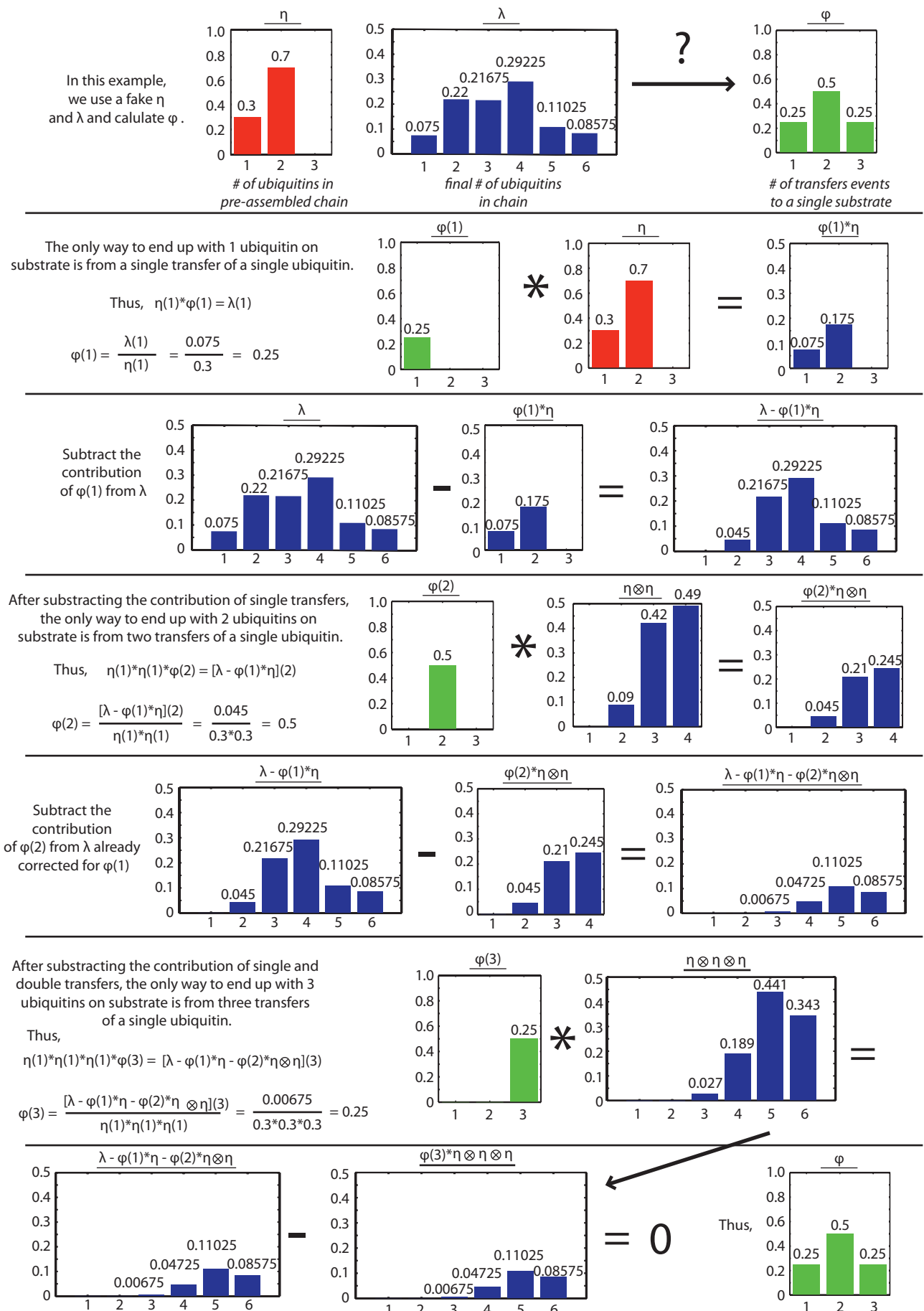


Supplementary Figure 2 | Calculation of λ . **a**, For clarity, Figure 1a is reproduced here. **b**, The distributions of products in reaction 3 were subtracted from the distribution of products in reaction 2 at each time point and then normalized. **c**, The average of the distributions shown in b is λ_{CycE} . **d**, The fractional amounts of each product ($S_1 - S_8$) that comprise the distribution λ_{CycE} . **e**, The fractional amounts of each product ($S_1 - S_{14}$) that comprise the distribution $\lambda_{\beta\text{-cat}}$. **f**, Calculation of the percent CycE bound to SCF^{Cdc4} at the beginning of the reaction, based on the reported K_d for binding of CycE to Cdc4.²¹ Combined with the kinetics of Fig. 1a the percent of productive encounters was calculated. **g**, Calculation of the percent $\beta\text{-Cat}$ bound to $\text{SCF}^{\beta\text{-TrCP}}$ at the beginning of the reaction, based on the reported K_d for binding of Ub- $\beta\text{-Cat}$ to $\beta\text{-TrCP}$.²² Combined with the kinetics of Fig. 1b the percent of productive encounters was calculated.

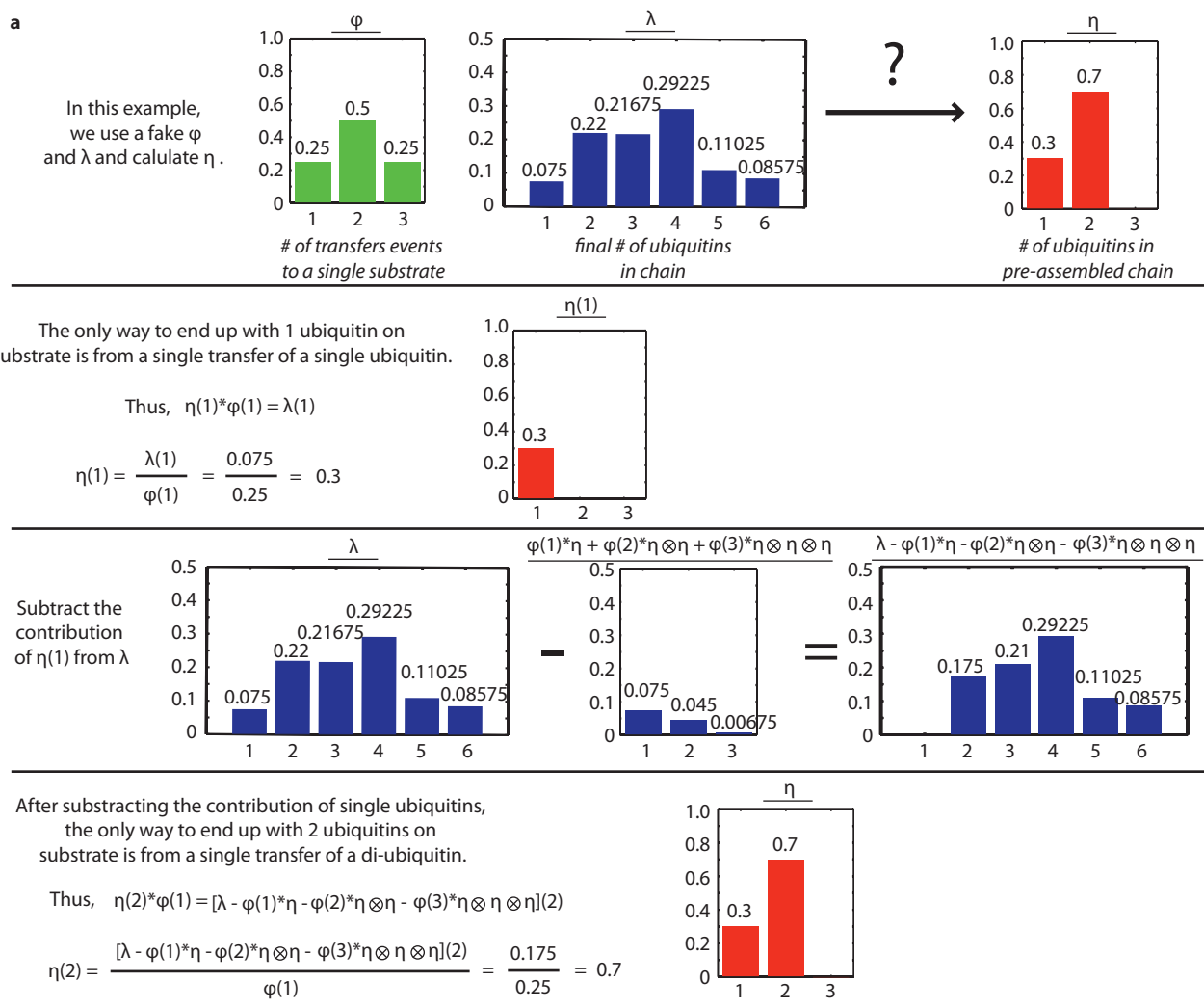


Supplementary Figure 3 | An example of calculating λ from η and ϕ . In this example, we assigned distributions to η and ϕ . To calculate λ , we took multiple convolutions of η with itself as governed by ϕ . In our example, 25% of substrates underwent one transfer, for which the η value determines that 30% were a single ubiquitin while 70% were diubiquitin. Thus, we weight the distribution η by the fraction of a single transfer, $\phi(1) * \eta$. 50% of substrates underwent two transfers. Each of these two transfers selects from the pool of pre-assembled chains, thus we must consider the convolution of η with itself ($\eta \otimes \eta$) and then weight it by the fraction that receive two transfers, $\phi(2) * \eta \otimes \eta$. This process is repeated for the all indexes of ϕ , each time adding an additional convolution. These weighted distributions sum to give λ .





Supplementary Figure 4 | An example of calculating ϕ from λ and η . Deconvolution took advantage of the constraints existing on the lowest index of λ . Here we used λ and η from the example in Supplementary Figure 3. The only way of creating the species in λ that has a single ubiquitin attached to substrate was by the single transfer of a single ubiquitin. Thus, $\phi(1)*\eta(1)$ equals $\lambda(1)$ and $\phi(1)$ is calculated by division. The contribution of $\phi(1)$ to λ was then calculated and subtracted from λ . The only way remaining to form $\lambda(2)$, is by two transfers of a single ubiquitin. Thus $\phi(2)$ equals $[\lambda - \phi(1)*\eta](2)/[\eta(1)*\eta(1)]$. This process is repeated until ϕ is revealed.



b Exponential normalized distributions of η with varying rate parameter α $e^{-\alpha * \eta(i)}$

α	$\eta(1)$	$\eta(2)$	$\eta(3)$	$\eta(4)$	$\eta(5)$	$\eta(6)$	$\eta(7)$	$\eta(8)$	Sum(η)
0.1	1.0000	0.0000	0.0000	0.0000	0.0000	0.0000	0.0000	0.0000	1.0000
0.2	0.9933	0.0067	0.0000	0.0000	0.0000	0.0000	0.0000	0.0000	1.0000
0.3	0.9643	0.0344	0.0012	0.0000	0.0000	0.0000	0.0000	0.0000	1.0000
0.4	0.9179	0.0753	0.0062	0.0005	0.0000	0.0000	0.0000	0.0000	1.0000
0.5	0.8647	0.1170	0.0158	0.0021	0.0003	0.0000	0.0000	0.0000	1.0000
0.6	0.8111	0.1532	0.0289	0.0055	0.0010	0.0002	0.0000	0.0000	1.0000
0.7	0.7604	0.1822	0.0437	0.0105	0.0025	0.0006	0.0001	0.0000	1.0000
0.8	0.7135	0.2044	0.0586	0.0168	0.0048	0.0014	0.0004	0.0001	1.0000
0.9	0.6709	0.2209	0.0727	0.0239	0.0079	0.0026	0.0009	0.0003	1.0000
1.0	0.6323	0.2326	0.0856	0.0315	0.0116	0.0043	0.0016	0.0006	1.0000

ϕ as given by the multiple weighted sums deconvolution of exponential η (above) and λ

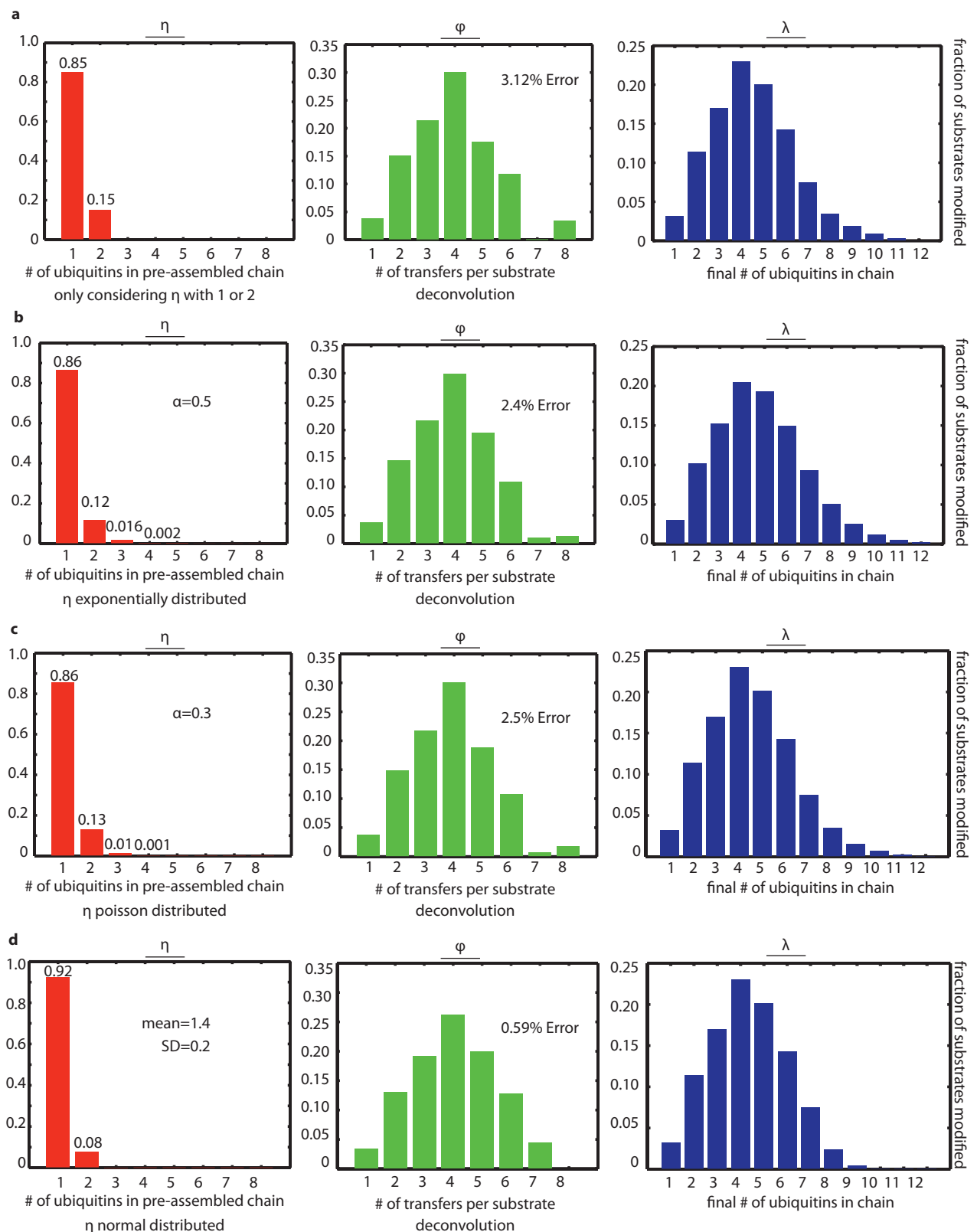
α	$\phi(1)$	$\phi(2)$	$\phi(3)$	$\phi(4)$	$\phi(5)$	$\phi(6)$	$\phi(7)$	$\phi(8)$	Sum(ϕ)
0.1	0.0320	0.1140	0.1700	0.2300	0.2010	0.1430	0.0750	0.0350	1.0000
0.2	0.0322	0.1153	0.1719	0.2328	0.2015	0.1420	0.0727	0.0334	1.0018
0.3	0.0332	0.1214	0.1805	0.2454	0.2032	0.1368	0.0619	0.0265	1.0089
0.4	0.0349	0.1322	0.1959	0.2682	0.2027	0.1255	0.0409	0.0171	1.0174
0.5	0.0370	0.1467	0.2161	0.2991	0.1946	0.1079	0.0098	0.0130	1.0241
0.6	0.0395	0.1641	0.2400	0.3365	0.1726	0.0860	-0.0321	0.0266	1.0332
0.7	0.0421	0.1839	0.2666	0.3799	0.1296	0.0657	-0.0878	0.0779	1.0579
0.8	0.0448	0.2059	0.2954	0.4290	0.0575	0.0580	-0.1661	0.1998	1.1244
0.9	0.0477	0.2299	0.3259	0.4839	-0.0531	0.0804	-0.2856	0.4476	1.2767
1.0	0.0506	0.2557	0.3578	0.5446	-0.2129	0.1586	-0.4812	0.9139	1.5870

Supplementary Figure 5 | An example of calculating η from λ and ϕ . **a**, This example is similar to that in Supplementary Figure 4. Here, each time we discover another value of η we must remember to subtract the multi-weighted convolutions (as in Supplementary Figure 3) of the incomplete η from λ . **b**, Shown is the explicit example of searching a normalized exponential distribution of η by varying the rate parameter α . When the deconvolution was performed with rate parameter $\alpha=0.5$, the first negative number appeared at $\phi(6)$. All larger rate parameters contain negative values. The error for this distribution was calculated as the difference in its sum from 1.

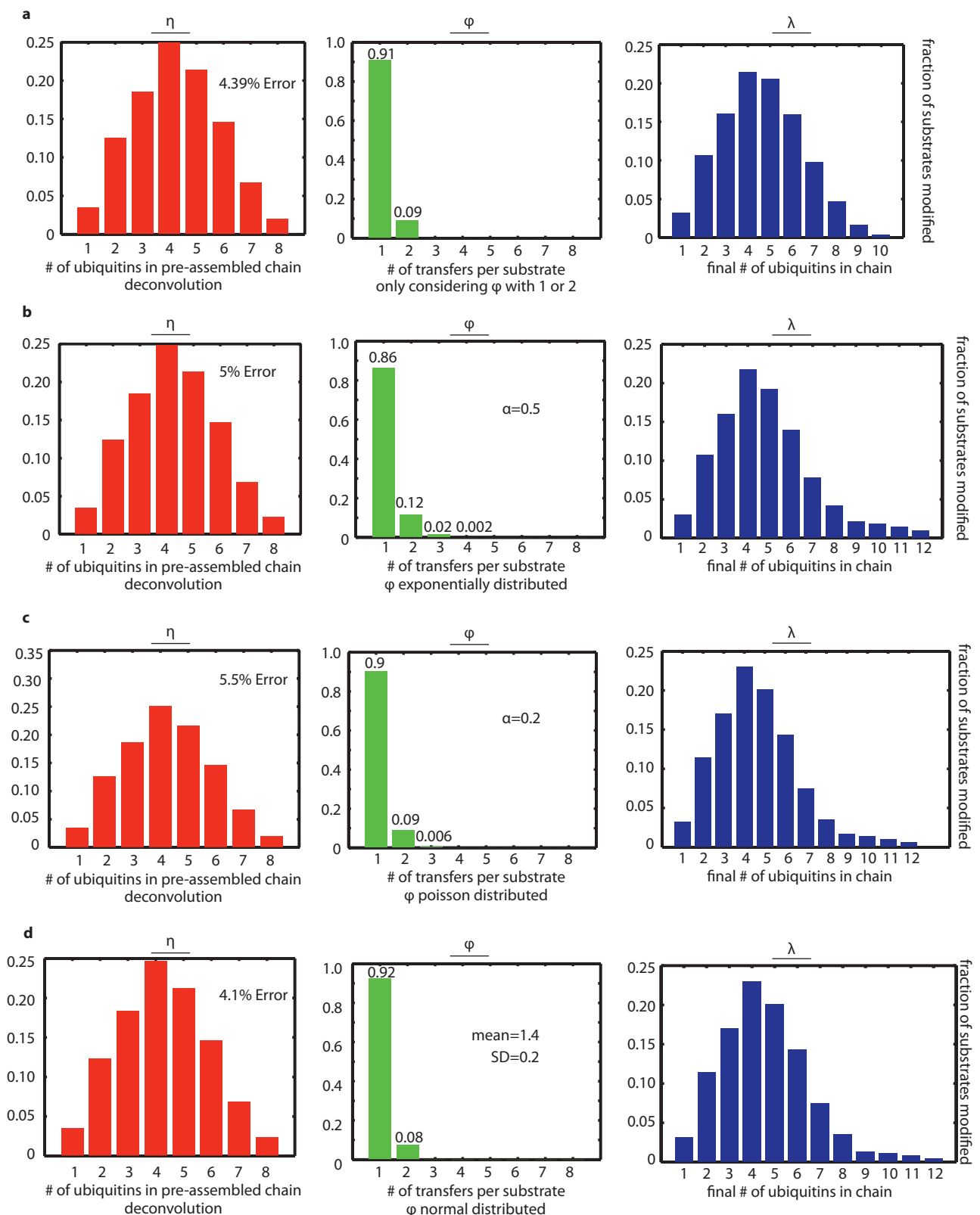
← Largest α without negative values ($\alpha=0.5$)

Difference between the Sum(ϕ) and 1 is the error.

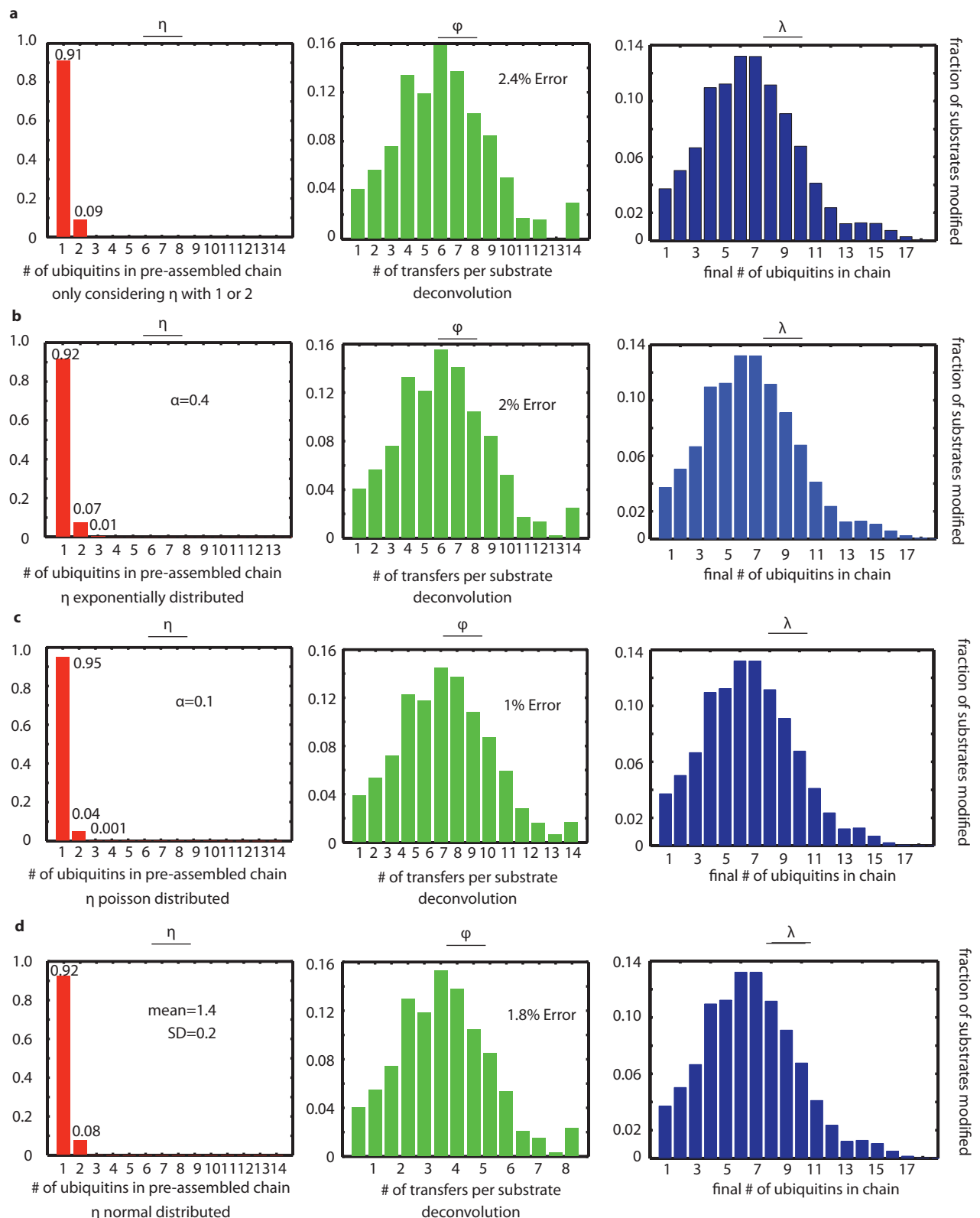
Error = 2.4%



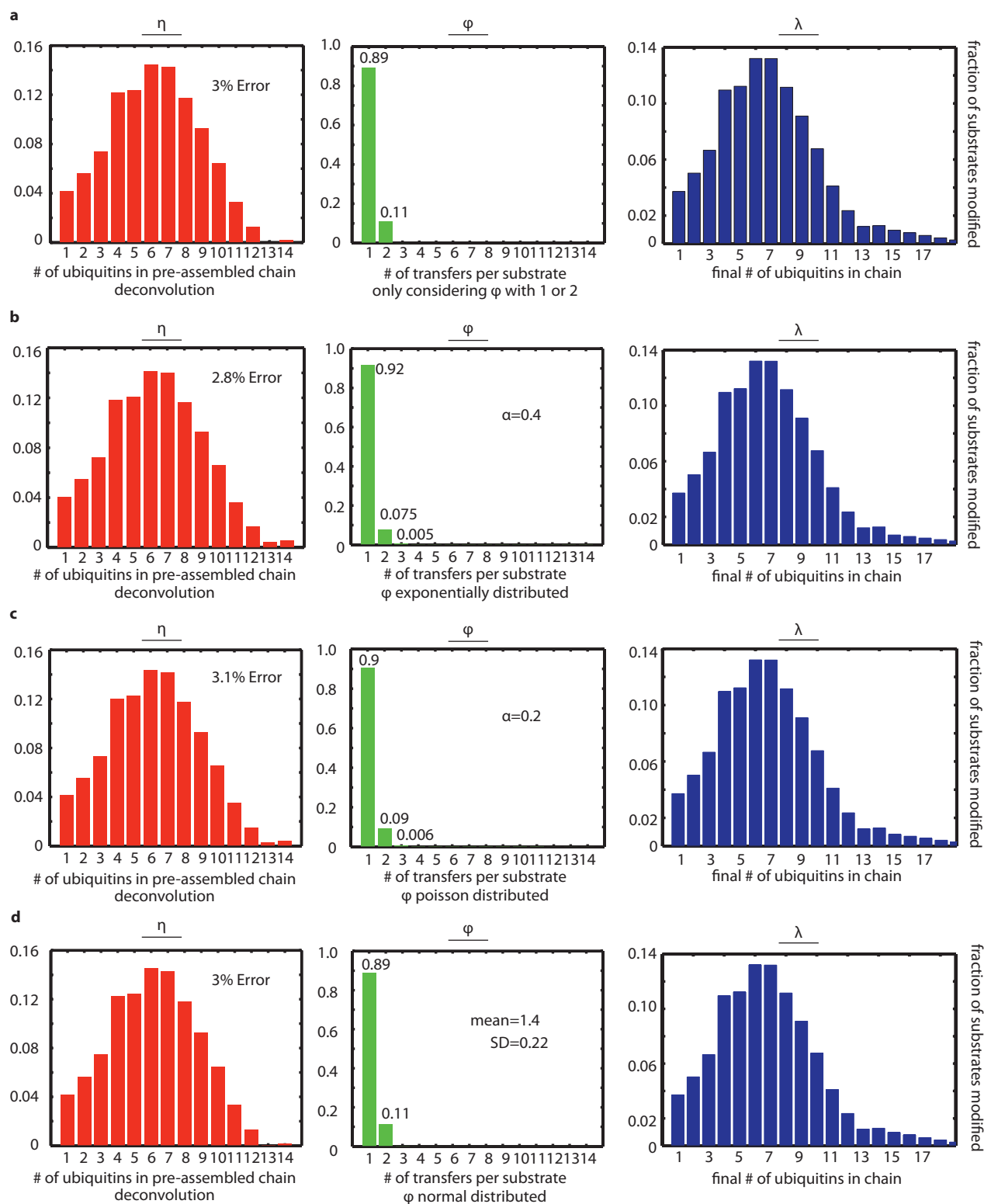
Supplementary Figure 6 | Deconvolution of ϕ from λ_{CycE} . **a**, Considering distributions of η that only contain $\eta(1)$ and $\eta(2)$, ϕ was calculated by deconvolution with λ_{CycE} . The distribution shown was that which deviated most from $\eta(1)=100\%$ whose ϕ did not contain values >1 or <0 and that when convoluted with ϕ , the sum fell within 0.95 and 1.05, or an error rate of $\pm 5\%$. **b**, Considering distributions of η that were exponentially distributed with rate parameter α . **c**, Considering distributions of η that were poisson distributed with average α . **d**, Considering distributions of η that were normal distributed varying the mean and SD. Random distributions were also considered (data not shown).



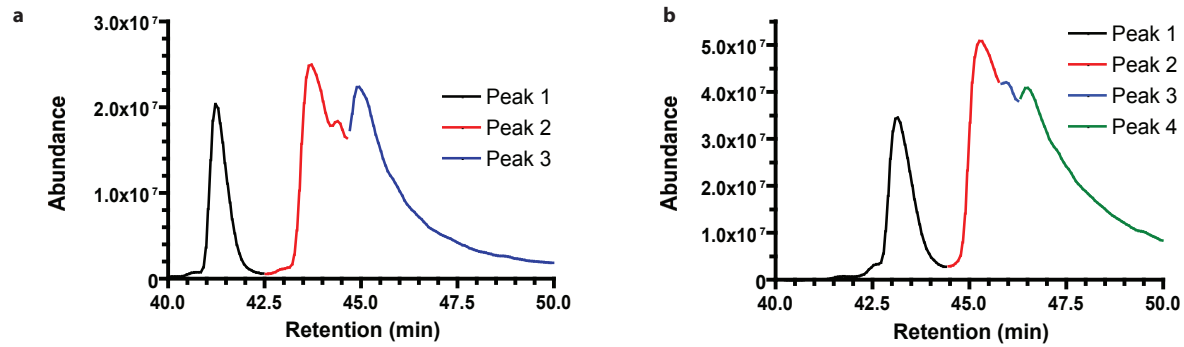
Supplementary Figure 7 | Deconvolution of η from λ_{cyc} . **a**, Considering distributions of ϕ that only contain $\phi(1)$ and $\phi(2)$, η was calculated by deconvolution with λ_{cyc} . The distribution shown was that which deviated most from $\phi(1)=100\%$ whose η did not contain values >1 or <0 and that when convoluted with η , the sum fell within 0.95 and 1.05, or an error rate of $\pm 5\%$. **b**, Considering distributions of ϕ that were exponentially distributed with rate parameter α . **c**, Considering distributions of ϕ that were poisson distributed with average α . **d**, Considering distributions of ϕ that were normal distributed varying the mean and SD. Random distributions were also considered (data not shown).



Supplementary Figure 8 | Deconvolution of ϕ from λ . **a**, Considering distributions of η that only contain $\eta(1)$ and $\eta(2)$, ϕ was calculated by deconvolution with $\lambda_{\text{B-Cat}}$. The distribution shown was that which deviated most from $\eta(1)=100\%$ whose ϕ did not contain values >1 or <0 and that when convoluted with ϕ , the sum fell within 0.95 and 1.05, or an error rate of $\pm 5\%$. **b**, Considering distributions of η that were exponentially distributed with rate parameter α . **c**, Considering distributions of η that were poisson distributed with average α . **d**, Considering distributions of η that were normal distributed varying the mean and SD. Random distributions were also considered (data not shown).



Supplementary Figure 9 | Deconvolution of η from λ . **a**, Considering distributions of ϕ that only contain $\phi(1)$ and $\phi(2)$, η was calculated by deconvolution with $\lambda_{\beta\text{-Cat}}$. The distribution shown was that which deviated most from $\phi(1)=100\%$ whose η did not contain values >1 or <0 and that when convoluted with η , the sum fell within 0.95 and 1.05, or an error rate of $\pm 5\%$. **b**, Considering distributions of ϕ that were exponentially distributed with rate parameter α . **c**, Considering distributions of ϕ that were poisson distributed with average α . **d**, Considering distributions of ϕ that were normal distributed varying the mean and SD. Random distributions were also considered (data not shown).

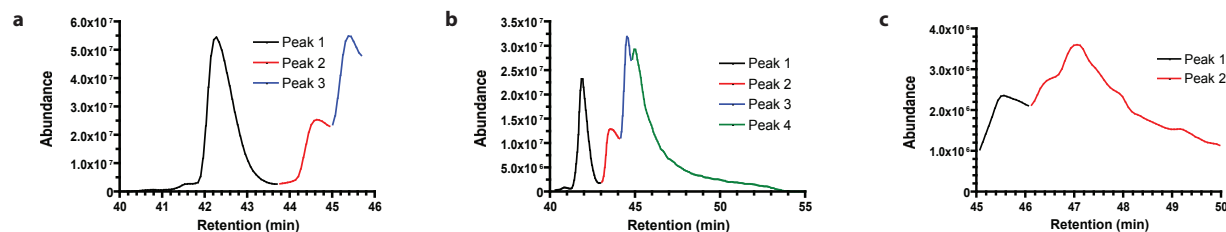


Protein	Mass (theoretical)	Mass (measured)	Abundance	Peak
Ubiquitin	8565	8565	1,250,158	1
Cdc34~Ub	40,792	40,792	838,665	2
		41,830	137,725	2
		40,787	204,375	3
		60,559	170,061	3
		104,033	147,021	3
		106,823	144,456	3
		88,303	142,422	3
		107,237	134,176	3
		80,790	134,085	3
		106,427	130,900	3
		89,100	125,780	3
		79,957	124,787	3

d

Protein	Mass (theoretical)	Mass (measured)	Abundance	Peak
Ubiquitin	8565	8564	1,448,614	1
Ub-DTT	8701	8701	627,263	1
Cdc34~Ub	40,792	40,789	2,267,926	2
Cdc34~Ub	40,792	40,790	1,217,040	3
Cdc34	32,245	32,242	145,616	3
Cdc34~Ub	40,792	40,788	471,765	4
Cdc34	32,245	32,243	326,504	4
		60,570	176,801	4
		80,775	156,325	4
		79,940	153,394	4
		60,129	144,097	4
		61,003	116,335	4
		61,460	112,311	4
		59,775	103,833	4
		79,121	97,101	4

Supplementary Figure 10 | Mass spectrometry analysis of Cdc34. **a**, Chromatograms of mass spectrometry analysis of reaction containing Uba1, yeast Cdc34 and ubiquitin in the presence of ATP. Where possible, species are identified and the masses are compared with the theoretical value. Peak 3 contains multiple species including Uba1 and impurities. The theoretical masses for Cdc34~Uba2 (49,338), Cdc34~Uba3 (57,886), Cdc34~Uba4 (66,433) are not observed. **b**, Chromatograms of mass spectrometry analysis of reaction containing Uba1, yeast Cdc34 and ubiquitin (Ub) in the presence of ATP and SCF^{Cdc4}. Where possible, species are identified and the masses are compared with the theoretical value. Peak 4 contains multiple species including E1 and impurities. **c**, Analysis of peaks from **a**. **d**, Analysis of peaks from **b**.



d

Protein	Mass (theoretical)	Mass (measured)	Abundance	Peak
Ub-DTT	8701	8701	4,004,748	1
Cdc34~Ub	40,792	40,790	856,005	2
Cdc34	32,245	32,243	2,104,438	3

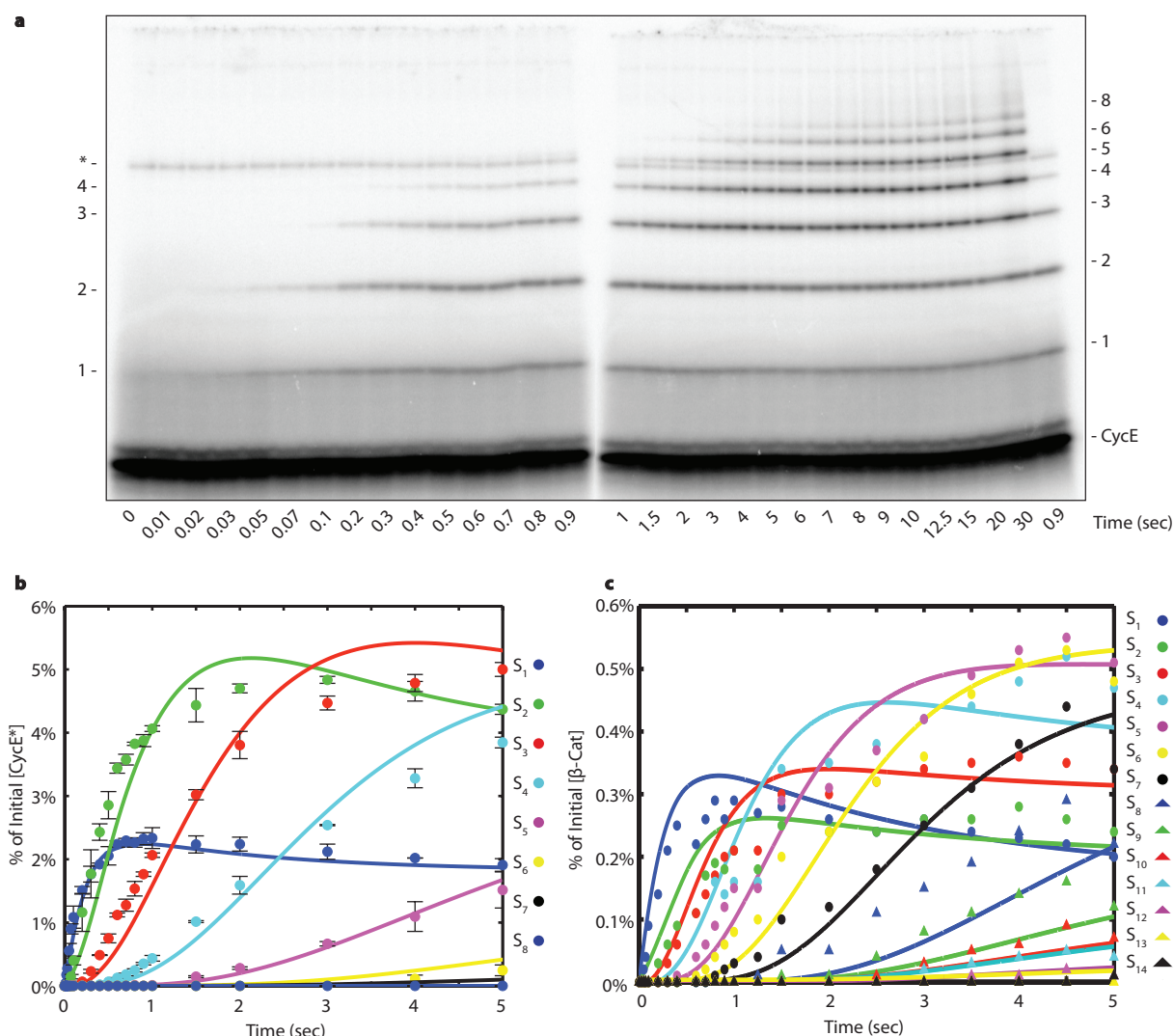
e

Protein	Mass (theoretical)	Mass (measured)	Abundance	Peak
Di-ubiquitin	17,111	17,093	1,219,060	1
Cdc34~Ub2	49,338	49,339	358,429	2
Cdc34	32,245	32,244	1,056,240	3
Cdc34	32,245	32,243	342,426	4
		114,412	141,956	4
		113,442	131,956	4
		55,481	113,943	4
		115,141	112,219	4
		55,890	111,557	4
		56,788	106,226	4
		112,563	87,983	4
		37,546	87,790	4
		44,326	81,153	4

f

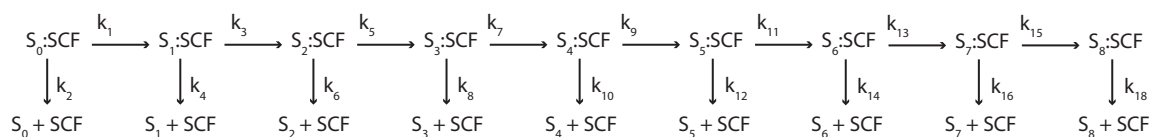
Protein	Mass (theoretical)	Mass (measured)	Abundance	Peak
		16,951	20,405	1
		40,816	13,500	1
		16,991	10,620	1
		16,977	9,508	1
		40,861	8524	1
		17,008	6,772	1
		41,838	6,612	1
		40,900	6,249	1
		36,023	6,204	1
		78,867	6,008	1
		109,318	20,828	2
		109,554	20,484	2
		98,618	19,802	2
		66,153	18,346	2
		61,032	18,301	2
		88,227	17,086	2
		37,291	15,688	2
		52,670	15,672	2
		64,288	15,270	2
		80,111	15,003	2

Supplementary Figure 11 | Mass spectrometry analysis of Cdc34 controls. **a**, Chromatograms of mass spectrometry analysis of reaction containing E1, Cdc34 and ubiquitin (Ub) in the presence of ATP, SCF and DTT. Where possible, species are identified and the masses are compared with the theoretical value. **b**, Chromatograms of mass spectrometry analysis of reaction containing E1, Cdc34 and K48 di-ubiquitin in the presence of ATP. Where possible, species are identified and the masses are compared with the theoretical value. Peak 4 contains multiple species including E1 and impurities. **c**, Chromatograms of mass spectrometry analysis of SCF^{Cdc34} in reaction buffer. **d**, Analysis of peaks from **a**. **e**, Analysis of peaks from **b**. **f**, Analysis of peaks from **c**.



Supplementary Figure 12 | Millisecond kinetics of a single encounter reaction. **a**, Samples from the same reaction shown in Fig. 2a were run on a 12-24% tricine gel to optimize detection and quantification of S2 and S5. The asterisk marks an unreactive contaminant of the labeled CycE. **b**, A zoomed plot of Fig. 3b up to 5 seconds. The error of each fit is shown in Supplementary Figure 14. **c**, A zoomed plot of Fig. 3e up to 5 seconds. The error of each fit is shown in Supplementary Figure 15.

Analytical Closed Form Solutions



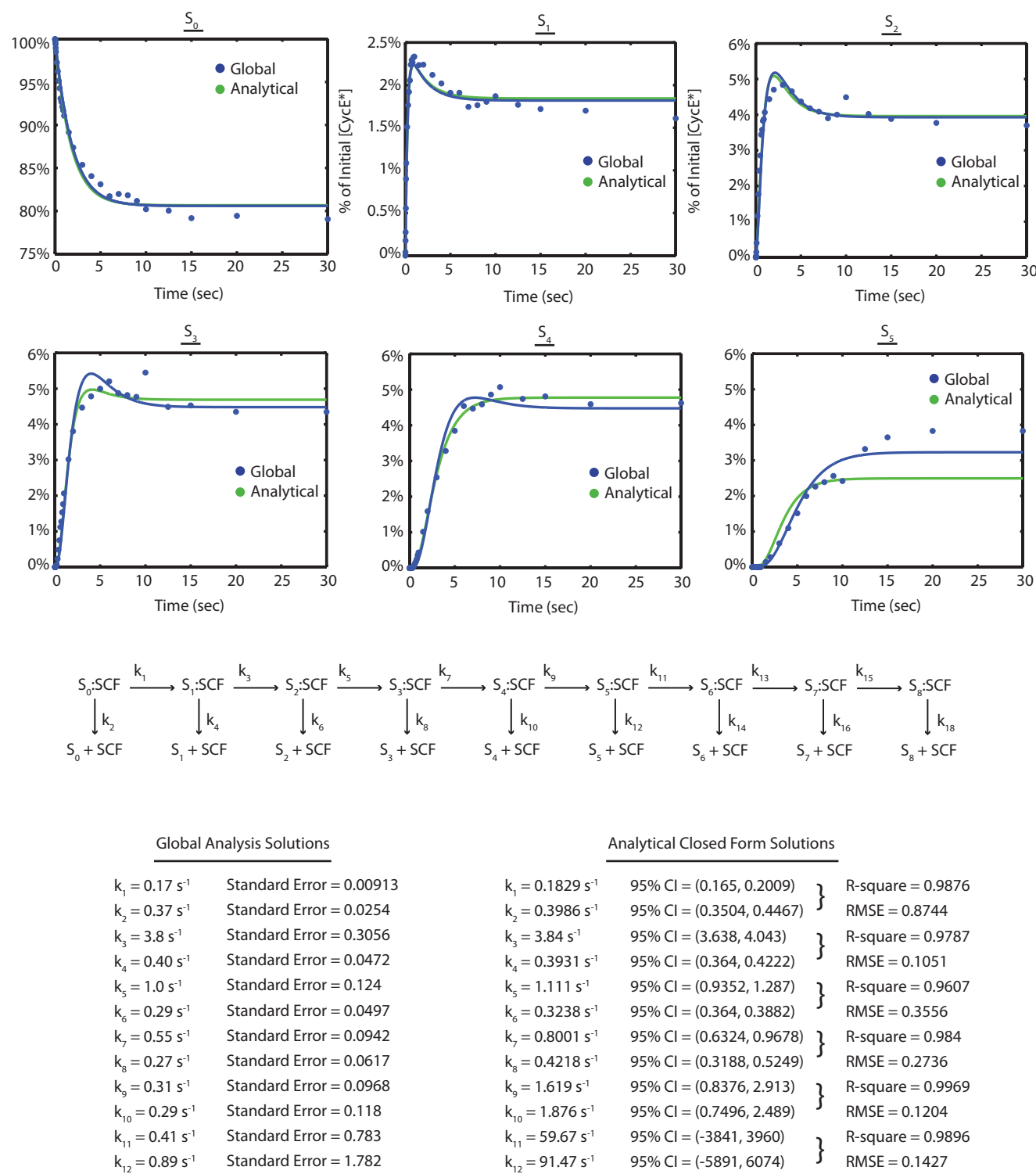
$$[SCF:S_0] = 61.5\% \text{ at } t=0$$

$$[S_0] = 61.5 \left(1 - \frac{k_2}{k_1+k_2} \right) e^{-(k_1+k_2)t} + 61.5 \frac{k_2}{k_1+k_2} + (100-61.5)$$

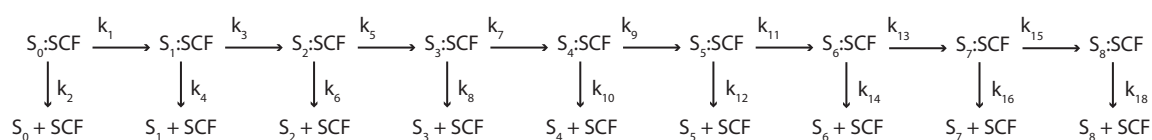
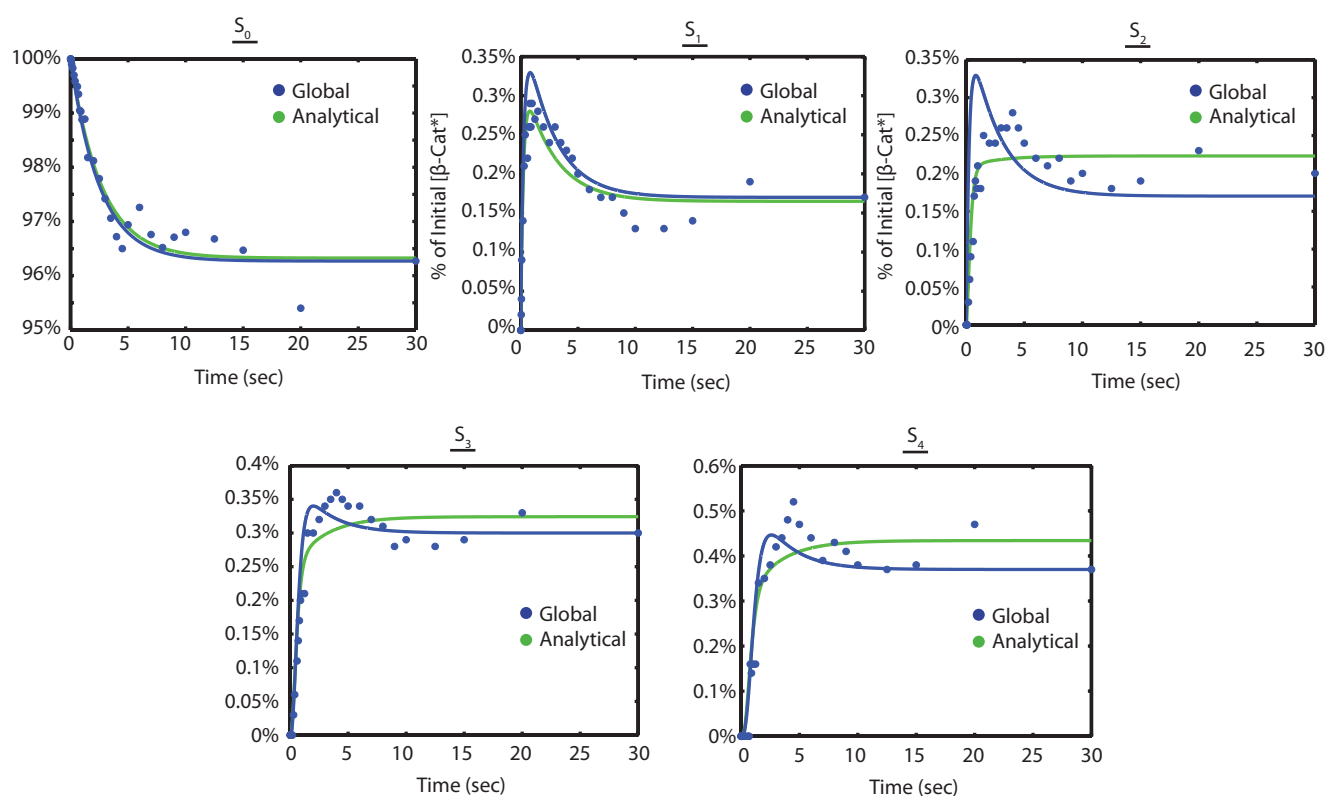
$$[S_1]_{\text{Total}} = 61.5 k_1 \left(\frac{e^{-(k_1+k_2)t}}{(k_3+k_4)-(k_1+k_2)} + \frac{e^{-(k_3+k_4)t}}{(k_1+k_2)-(k_3+k_4)} \right) + 61.5 \left(\frac{k_1}{k_1+k_2} \right) \left(\frac{k_4}{k_3+k_4} \right) \left(1 - \frac{(k_3+k_4)e^{-(k_1+k_2)t}}{(k_3+k_4)-(k_1+k_2)} - \frac{(k_1+k_2)e^{-(k_3+k_4)t}}{(k_1+k_2)-(k_3+k_4)} \right)$$

$$\begin{aligned}
 [S_2]_{\text{Total}} = & 61.5 k_1 k_3 \left(\frac{e^{-(k_1+k_2)t}}{((k_3+k_4)-(k_1+k_2))((k_5+k_6)-(k_1+k_2))} + \frac{e^{-(k_3+k_4)t}}{((k_1+k_2)-(k_3+k_4))((k_5+k_6)-(k_3+k_4))} + \frac{e^{-(k_5+k_6)t}}{((k_1+k_2)-(k_5+k_6))((k_3+k_4)-(k_5+k_6))} \right) \\
 & + 61.5 \left(\frac{k_1}{k_1+k_2} \right) \left(\frac{k_3}{k_3+k_4} \right) \left(\frac{k_6}{k_5+k_6} \right) \left(1 - \frac{(k_3+k_4)(k_5+k_6)e^{-(k_1+k_2)t}}{((k_3+k_4)-(k_1+k_2))((k_5+k_6)-(k_1+k_2))} - \frac{(k_1+k_2)(k_5+k_6)e^{-(k_3+k_4)t}}{((k_1+k_2)-(k_3+k_4))((k_5+k_6)-(k_3+k_4))} - \frac{(k_1+k_2)(k_3+k_4)e^{-(k_5+k_6)t}}{((k_1+k_2)-(k_5+k_6))((k_3+k_4)-(k_5+k_6))} \right) \\
 [S_{n/2}]_{\text{Total}} = & 61.5 k_1 k_3 \dots k_{n-1} \left(\frac{e^{-(k_1+k_2)t}}{((k_3+k_4)-(k_1+k_2))((k_5+k_6)-(k_1+k_2)) \dots ((k_{n-1}+k_n)-(k_1+k_2))} + \frac{e^{-(k_3+k_4)t}}{((k_1+k_2)-(k_3+k_4))((k_5+k_6)-(k_3+k_4)) \dots ((k_{n-1}+k_n)-(k_3+k_4))} \right. \\
 & \left. + \dots + \frac{e^{-(k_{n-1}+k_n)t}}{((k_1+k_2)-(k_{n-1}+k_n))((k_3+k_4)-(k_{n-1}+k_n)) \dots ((k_{n-3}+k_{n-2})-(k_{n-1}+k_n))} \right) \\
 & + 61.5 \left(\frac{k_1}{k_1+k_2} \right) \left(\frac{k_3}{k_3+k_4} \right) \dots \left(\frac{k_n}{k_{n-1}+k_n} \right) \left(1 - \frac{(k_3+k_4)(k_5+k_6) \dots (k_{n-1}+k_n)e^{-(k_1+k_2)t}}{((k_3+k_4)-(k_1+k_2))((k_5+k_6)-(k_1+k_2)) \dots ((k_{n-1}+k_n)-(k_1+k_2))} - \frac{(k_1+k_2)(k_5+k_6) \dots (k_{n-1}+k_n)e^{-(k_3+k_4)t}}{((k_1+k_2)-(k_3+k_4))((k_5+k_6)-(k_3+k_4)) \dots ((k_{n-1}+k_n)-(k_3+k_4))} \right. \\
 & \left. - \frac{(k_1+k_2)(k_3+k_4) \dots (k_{n-3}+k_{n-2})e^{-(k_{n-1}+k_n)t}}{((k_1+k_2)-(k_{n-1}+k_n))((k_3+k_4)-(k_{n-1}+k_n)) \dots ((k_{n-3}+k_{n-2})-(k_{n-1}+k_n))} \right)
 \end{aligned}$$

Supplementary Figure 13 | Closed form solutions to a kinetic model of a single encounter reaction with $\eta(1)=100\%$. The analytical solutions were calculated using the method of Laplace transforms. Each new species contributed two new rate constants to the overall scheme.



Supplementary Figure 14 | Comparison of rate constants estimated from analytical solutions and global regression for CycE. Comparison of the analytical and globally refined rate constants revealed that the global analysis helped to correct for the error accumulation in the analytical regression.



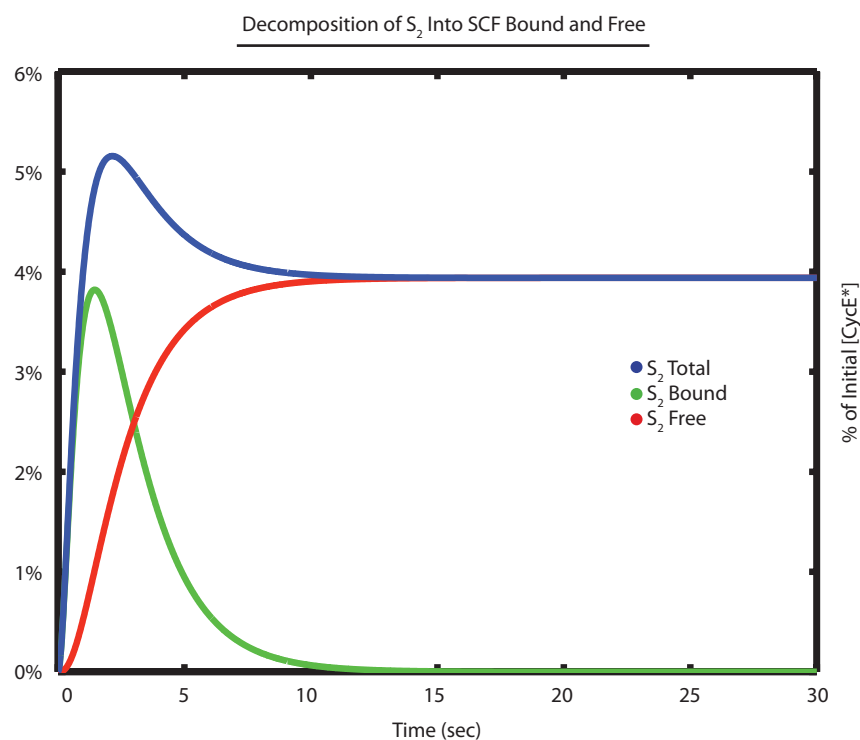
Global Analysis Solutions

$k_1 = 0.03 \text{ s}^{-1}$	Standard Error = 0.00261
$k_2 = 0.363 \text{ s}^{-1}$	Standard Error = 0.0313
$k_3 = 3.58 \text{ s}^{-1}$	Standard Error = 0.627
$k_4 = 0.171 \text{ s}^{-1}$	Standard Error = 0.0299
$k_5 = 4.45 \text{ s}^{-1}$	Standard Error = 1.1
$k_6 = 0.265 \text{ s}^{-1}$	Standard Error = 0.0658
$k_7 = 3.22 \text{ s}^{-1}$	Standard Error = 0.802
$k_8 = 0.315 \text{ s}^{-1}$	Standard Error = 0.0786
$k_9 = 2 \text{ s}^{-1}$	Standard Error = 0.481
$k_{10} = 0.275 \text{ s}^{-1}$	Standard Error = 0.0661
$k_{11} = 1.63 \text{ s}^{-1}$	Standard Error = 0.420
$k_{12} = 0.372 \text{ s}^{-1}$	Standard Error = 0.0959
$k_{13} = 1.21 \text{ s}^{-1}$	Standard Error = 0.382
$k_{14} = 0.395 \text{ s}^{-1}$	Standard Error = 0.125
$k_{15} = 1.01 \text{ s}^{-1}$	Standard Error = 0.571
$k_{16} = 0.467 \text{ s}^{-1}$	Standard Error = 0.241

Analytical Closed Form Solutions

$k_1 = 0.02839 \text{ s}^{-1}$	95% CI = (0.02413, 0.03266)	} R-square = 0.9634
$k_2 = 0.3463 \text{ s}^{-1}$	95% CI = (0.2797, 0.413)	
$k_3 = 4.098 \text{ s}^{-1}$	95% CI = (3.757, 4.44)	} R-square = 0.9112
$k_4 = 0.1926 \text{ s}^{-1}$	95% CI = (0.1628, 0.2224)	
$k_5 = 5.849 \text{ s}^{-1}$	95% CI = (4.942, 6.755)	} R-square = 0.8988
$k_6 = 0.1926 \text{ s}^{-1}$	95% CI = (0.3149, 0.479)	
$k_7 = 4.278 \text{ s}^{-1}$	95% CI = (3.614, 4.943)	} R-square = 0.9488
$k_8 = 0.4682 \text{ s}^{-1}$	95% CI = (0.3779, 0.5585)	
$k_9 = 2.927 \text{ s}^{-1}$	95% CI = (2.092, 3.763)	} R-square = 0.9209
$k_{10} = 0.5024 \text{ s}^{-1}$	95% CI = (0.3304, 0.6743)	
		RMSE = 0.05625

Supplementary Figure 15 | Comparison of rate constants estimated from analytical solutions and global regression for β -Cat. Comparison of the analytical and globally refined rate constants revealed that the global analysis helped to correct for the error accumulation in the analytical regression. The error for the β -Cat regressions are higher versus the CycE regression because of reduced fraction of substrate converted.



$$\begin{aligned}
 [S_2]_{\text{Total}} = [S_2]_{\text{bound}} + [S_2]_{\text{free}} = & 61.5 k_1 k_3 \left(\frac{e^{-(k_1+k_2)t}}{((k_3+k_4)-(k_1+k_2))((k_5+k_6)-(k_1+k_2))} + \frac{e^{-(k_3+k_4)t}}{((k_1+k_2)-(k_3+k_4))((k_5+k_6)-(k_3+k_4))} + \frac{e^{-(k_5+k_6)t}}{((k_1+k_2)-(k_5+k_6))((k_3+k_4)-(k_5+k_6))} \right) \\
 & + 61.5 \left(\frac{k_1}{k_1+k_2} \right) \left(\frac{k_3}{k_3+k_4} \right) \left(\frac{k_6}{k_5+k_6} \right) \left(1 - \frac{(k_3+k_4)(k_5+k_6)e^{-(k_1+k_2)t}}{((k_3+k_4)-(k_1+k_2))((k_5+k_6)-(k_1+k_2))} - \frac{(k_1+k_2)(k_5+k_6)e^{-(k_3+k_4)t}}{((k_1+k_2)-(k_3+k_4))((k_5+k_6)-(k_3+k_4))} - \frac{(k_1+k_2)(k_3+k_4)e^{-(k_5+k_6)t}}{((k_1+k_2)-(k_5+k_6))((k_3+k_4)-(k_5+k_6))} \right)
 \end{aligned}$$

Supplementary Figure 16 | Overshoot behavior reveals flux through each species. Using the analytical solutions, the overshoot behavior was directly correlated to the amount of flux through each species. Each curve may be dissected into the substrate that was bound to SCF or free at the time of quench. The sum of these two species gives the measured curve.